Cell Reports
Medicine

Article

Brown adipose tissue is associated with healthier body fat distribution and metabolic benefits independent of regional adiposity

Graphical abstract

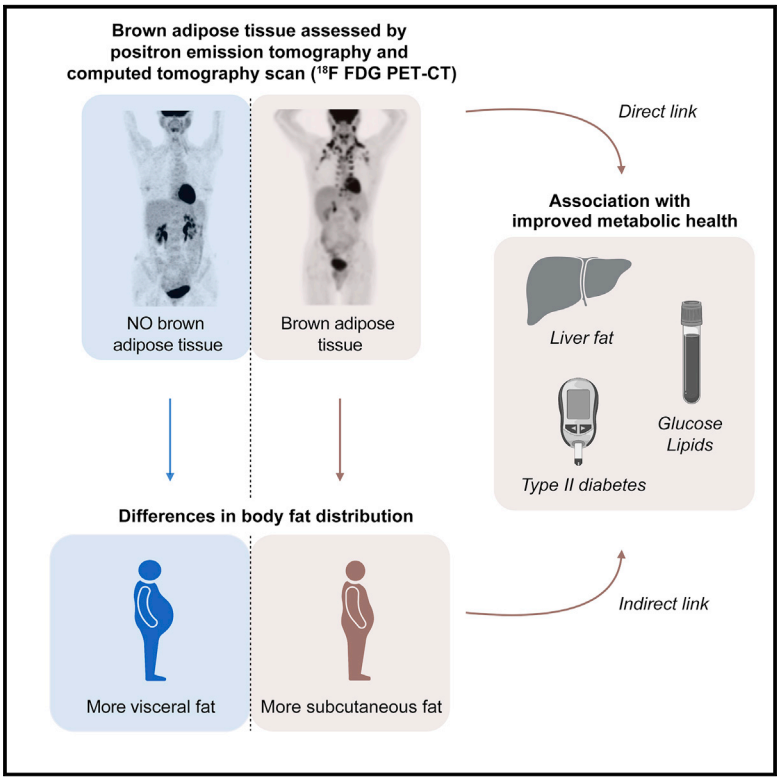

Highlights

- Brown adipose tissue is associated with more subcutaneous and less visceral fat
- Brown adipose tissue is associated with health independent of fat distribution
- Brown adipose tissue is associated with less liver fat and type 2 diabetes
- Brown adipose tissue is most beneficial in individuals with central obesity

Authors

Andreas G. Wibmer, Tobias Becher, Mahmoud Eljalby, ..., Roger Vaughan, Heiko Schöder, Paul Cohen

Correspondence

schoderh@mskcc.org (H.S.), pcohen@rockefeller.edu (P.C.)

In brief

Wibmer et al. report that brown adipose tissue is associated with a healthier body fat distribution and less central obesity and also associated independently with surrogate parameters of metabolic health and decreased liver fat accumulation. These observations are most prominent in individuals with central obesity.

Wibmer et al., 2021, Cell Reports Medicine 2, 100332
July 20, 2021
https://doi.org/10.1016/j.xcrm.2021.100332

CellPress

Cell Reports Medicine

CellPress
OPEN ACCESS

Article

Brown adipose tissue is associated with healthier body fat distribution and metabolic benefits independent of regional adiposity

Andreas G. Wibmer,[1,7] Tobias Becher,[2,3,4,7] Mahmoud Eljalby,[2,6] Audrey Crane,[2] Pamela Causa Andrieu,[1] Caroline S. Jiang,[5] Roger Vaughan,[5,6] Heiko Schöder,[1,8,*] and Paul Cohen[2,8,9,*]

[1]Department of Radiology, Memorial Sloan Kettering Cancer Center, New York, NY, USA
[2]Laboratory of Molecular Metabolism, The Rockefeller University, New York, NY, USA
[3]DZHK (German Centre for Cardiovascular Research), Partner Site Heidelberg/Mannheim, Mannheim, Germany
[4]First Department of Medicine (Division of Cardiology), University Medical Center Mannheim, Mannheim, Germany
[5]Center for Clinical and Translational Science, The Rockefeller University, New York, NY, USA
[6]Weill Cornell Medicine, New York, NY, USA
[7]These authors contributed equally
[8]These authors contributed equally
[9]Lead contact
*Correspondence: schoderh@mskcc.org (H.S.), pcohen@rockefeller.edu (P.C.)
https://doi.org/10.1016/j.xcrm.2021.100332

SUMMARY

The association of brown adipose tissue (BAT) and body fat distribution and their combined effects on metabolic health in humans remains unknown. Here, we retrospectively identify individuals with and without BAT on ^{18}F-fluorodeoxyglucose (^{18}F-FDG) positron emission tomography (PET)/computed tomography (CT) and assemble a propensity score-matched study cohort to compare body fat distribution and determine its role in mediating the benefits of brown fat. We find that BAT is associated with lower amounts of visceral adipose tissue and higher amounts of subcutaneous adipose tissue, resulting in less central obesity. In addition, BAT is independently associated with lower blood glucose and white blood cell count, improved lipids, lower prevalence of type 2 diabetes mellitus, and decreased liver fat accumulation. These observations are most prominent in individuals with central obesity. Our results support a role of BAT in protection from visceral adiposity and improved metabolic health.

INTRODUCTION

Obesity affects over 40% of American adults[1] and is expected to reach a prevalence of 48.9% by 2030.[2] Moreover, over 1 billion adults worldwide are predicted to be obese by 2030. These trends are a major public health concern because obesity and its sequelae contribute to increased morbidity, mortality, and healthcare costs.[3]

White adipose tissue (WAT), found in subcutaneous and visceral depots, stores excess triglycerides and accounts for increased body weight in states of positive energy balance.[4] Although subcutaneous WAT (SAT) is thought to be relatively benign[5,6] or even beneficial,[7] visceral WAT (VAT) has been implicated in metabolic dysfunction and insulin resistance.[8] Even more so than excess total body weight, visceral adiposity confers increased risk of coronary heart disease, type 2 diabetes mellitus (T2DM), certain types of cancer, and overall mortality.[9–14]

Recently, positron emission tomography (PET) and computed tomography (CT) imaging with ^{18}F-fluorodeoxyglucose (^{18}F-FDG) have been applied widely to identify brown adipose tissue (BAT) and quantify its activity in human adults.[15–18] BAT is characterized by expression of uncoupling protein 1 (UCP1), which is located in the inner mitochondrial membrane and facilitates a futile cycle, resulting in energy dissipation in the form of heat.[19–21] This exothermic process is fueled by increased glucose and fatty acid metabolism, suggesting that activation of BAT may result in decreased storage of calories in WAT and might therefore mitigate obesity and its harmful sequelae.[22–24] Individuals with BAT exhibit improved measures of glucose and lipid metabolism and a lower prevalence of cardiometabolic disease.[25–28] However, it still remains unclear how BAT mediates these beneficial effects.

Previous studies found an association between BAT and body fat distribution,[29–32] suggesting the possibility that healthier WAT distribution may mediate improved cardiometabolic outcomes in individuals with BAT. However, interpretation of these data is challenging because of small sample sizes and comparisons with unmatched controls, limiting the ability to make conclusions about whether BAT is linked to white fat distribution. It is also possible that BAT may improve metabolic outcomes independent of body fat distribution. In this study, we addressed this question in a large, propensity score-matched human cohort. Our findings suggest a more salutary

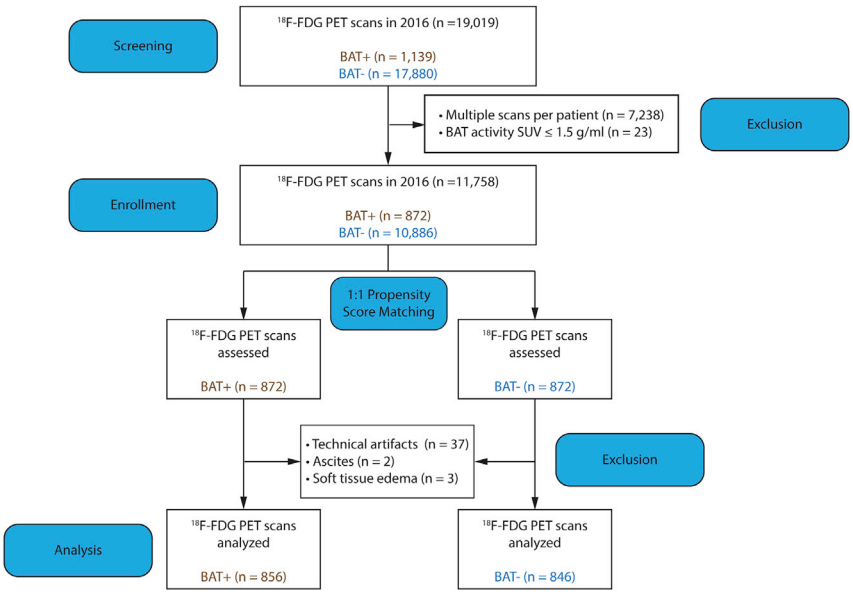

Figure 1. Flowchart of study participant selection

Shown is an outline of screening, enrollment, 1:1 propensity score matching, and derivation of the analysis cohort from all individuals age 18 and above who received a ^{18}F-FDG PET/CT scan in 2016.

pattern of body fat distribution in individuals with BAT as well as improved metabolic outcomes independent of effects on body fat distribution.

RESULTS AND DISCUSSION

Study cohort selection

We previously showed that BAT is associated with beneficial cardiometabolic effects;[25] however, the extent to which these effects might depend on WAT distribution is unknown. To assess the relationship between BAT and WAT distribution, we examined all 19,019 ^{18}F-FDG PET/CT scans performed at Memorial Sloan Kettering Cancer Center (MSKCC) in 2016 (Figure 1). These scans were performed to determine cancer diagnosis and stage as well as to monitor treatment response. It is the protocol at MSKCC to comment on BAT status in each study, and we have previously validated the accuracy of this reporting.[25] For individuals with BAT (BAT+ group), the first study revealing the presence of BAT was selected as the index scan. If an individual did not have any detectable BAT on any of their scans (BAT− group), then the earliest scan was designated the index scan.[25] Only the index scan was used for further analysis, excluding a total of 7,238 studies that represented multiple scans of the same individual (Figure 1). An additional 23 scans did not meet the Brown Adipose Reporting Criteria in Imaging Studies (BARCIST 1.0) criteria for BAT activity (standardized uptake value [SUV] > 1.5 g/mL)[33] and were excluded (Figure 1).

Of the remaining 11,758 individuals who met inclusion and exclusion criteria, 10,886 (92.6%) were BAT−, and 872 (7.4%) were BAT+ (Figure 1). To minimize baseline differences between BAT− and BAT+ individuals, we applied 1:1 propensity score matching using age, gender, body mass index (BMI), and ambient temperature in the month of the scan as matching variables to derive a study cohort for analysis (Figure S1). Each of these variables has been shown previously to be associated with brown fat prevalence and activity.[25,34,35] We then measured body fat distribution in the propensity score-matched study cohort. For this purpose, the CT scan that was obtained as part of ^{18}F-FDG PET/CT imaging was used to determine SAT and VAT distribution at the L3/L4 lumbar level. Analysis of the CT scans revealed that 42 subjects in the propensity score-matched study cohort had scans with significant technical artifacts (e.g., ascites or soft tissue edema) that interfered with quantification of abdominal WAT, resulting in their exclusion and leaving a final cohort of 856 BAT+ and 846 BAT− individuals for analysis (Figure 1).

Cohort characteristics and body fat distribution

After propensity score matching, there were no significant differences between BAT− and BAT+ individuals in age (49.5 years versus 49.0 years, respectively; $p = 0.4527$), gender (77.2% versus 76.6% females, respectively; $p = 0.8319$), BMI (24.7 kg/m^2 versus 24.9 kg/m^2, respectively; $p = 0.6204$), or ambient temperature in the month of the scan (12.5°C versus 12.5°C, respectively; $p = 0.9867$) (Table 1).

Similar to the observations for the entire cohort with available ^{18}F-FDG PET/CTs between 2009 and 2018 that were reported previously,[25] BAT+ individuals in the subgroup assembled for this study showed a significantly lower prevalence of T2DM (6.1% versus 10.4% in the BAT− group, $p = 0.0012$), lower blood glucose levels (87.0 mg/dL versus 90.0 mg/dL in the BAT− group, $p < 0.0001$), higher high-density lipoprotein (HDL) levels (53.5 mg/dL versus 47.0 mg/dL in the BAT− group, $p = 0.004$), lower triglyceride levels (98.0 mg/dL versus 129.0 mg/dL in the BAT− group, $p = 0.0027$), and lower white blood cell (WBC) count (a metric for systemic inflammation; 5.8×10^9 cells/L versus 6.7×10^9 cells/L in the BAT− group, $p < 0.0001$). Low-density lipoprotein (LDL) and total cholesterol were not significantly different between the two groups (Table 1).

On the same PET/CT scans that were examined for BAT status, we quantified waist circumference and SAT and VAT areas and determined the SAT:VAT area ratio as a measure of central adiposity (Figure 2A). To validate our measurements against the commonly used girth measurement,[36,37] we assessed available physical girth measurements against the CT-derived waist circumference and observed a strong and significant correlation between the two metrics ($r = 0.8257$, $p < 0.0001$) (Figure S2). When assessing associations between BMI and the two WAT depots, BMI correlated significantly with SAT area ($r = 0.8348$, $p < 0.0001$) and VAT area ($r = 0.6769$, $p < 0.0001$) but not with

Table 1. Characteristics of individuals with and without brown fat on ^{18}F-FDG PET/CT after propensity score matching

Parameter	BAT (BAT−) (n = 846)	BAT (BAT+) (n = 856)	Value
Clinical characteristics			
Age, mean (SD)	49.5 (15.3)	49.0 (15.8)	0.4527
Gender, no. (%)			0.8319
Female	653 (77.2)	656 (76.6)	
Male	193 (22.8)	200 (23.4)	
BMI, median (IQR)	24.7 (21.7–28.4)	24.9 (22.0–28.0)	0.6204
Ambient temperature in °C in month of scan, mean (SD)	12.5 (8.4)	12.5 (8.4)	0.9867
Race, no. (%)			0.0240
Asian	88 (10.4)	58 (6.8)	
African American	78 (9.2)	99 (11.6)	
Caucasian	596 (70.4)	603 (70.4)	
Other or unknown	84 (9.9)	96 (11.2)	
Ethnicity, no. (%)			0.0511
Hispanic	70 (8.3)	89 (10.4)	
Non-Hispanic	769 (90.9)	751 (87.7)	
Unknown	7 (0.8)	16 (1.9)	
Fat distribution, median (IQR)			
Waist circumference on CT, cm	86.9 (78.6–96.3)	87.7 (79.3–96.2)	0.6740
VAT, area cm^2	74.3 (39.5–128.8)	68.2 (39.5–111.0)	0.0307
SAT, area cm^2	176.0 (113.3–257.0)	188.0 (127.0–272.3)	0.0036
SAT/VAT ratio	2.4 (1.5–3.4)	2.7 (1.9–4.1)	<0.0001
Laboratory values, median (IQR)			
Glucose, mg/dL	90.0 (82.3–97.8)	87.0 (80.0–96.0)	<0.0001
LDL, mg/dL	108.5 (80.0–142.5)	110.0 (84.5–137.5)	0.7605
HDL, mg/dL	47.0 (34.0–63.0)	53.5 (43.0–73.0)	0.004
Cholesterol, mg/dL	192.0 (152.0–223.5)	196.0 (160.0–220.0)	0.5081
Triglycerides, mg/dL	129.0 (87.0–177.5)	98.0 (75.0–136.0)	0.0027
WBC count, 10^9 cells/L	6.7 (5.3–8.2)	5.8 (4.4–7.5)	<0.0001
Metabolic outcomes			
Liver density, HU, median (IQR)	58.6 (53.4–62.9)	60.3 (55.7–64.3)	<0.0001
T2DM, no. (%)	88 (10.4)	52 (6.1)	0.0012

BAT, brown adipose tissue; BMI, body mass index; HU, Hounsfield unit; SAT, subcutaneous adipose tissue; SD, standard deviation; IQR, interquartile range, VAT, visceral adipose tissue.

the SAT:VAT ratio (r = −0.0241, p = 0.3212) (Figures 2B and 2C). The distribution of the SAT:VAT ratio was right-skewed (Figure 2D), as described previously.[38,39]

We observed statistically significant but diminished correlations between VAT area and blood glucose (r = 0.2435, p < 0.0001), HDL (r = −0.2402, p = 0.0005), triglycerides (r = 0.2799, p < 0.0001), and WBC count (r = 0.1795, p < 0.0001) but not with total cholesterol or LDL levels (Table S1).[40] In contrast, SAT area was correlated significantly but weakly with blood glucose (r = 0.07041, p = 0.0039) and WBC count (r = 0.0738, p = 0.0028) but not with total cholesterol, triglycerides, LDL, or HDL levels (Table S1). To adjust for known confounders that may underpin these correlations, we used a multivariable linear regression model adjusted for SAT and VAT area in addition to age, gender, and BMI. Consistent with the literature, VAT area was identified as an independent positive predictor of blood glucose, triglycerides, and WBC count and negative predictor of HDL (Table S2), whereas SAT area was an independent negative predictor of blood glucose only (Table S2).[40] Our findings confirm previous reports that VAT, much more than SAT, is the main driver of comorbid metabolic disease.[6–8]

BAT is associated with a reduction in central adiposity

We then investigated whether BAT status is associated with body fat distribution. Although we observed no difference between the matched BAT− and BAT+ groups in BMI or waist circumference (86.9 versus 87.7 cm, respectively; p = 0.6740), BAT+ status was associated with a significantly decreased VAT area (74.3 versus 68.2 cm^2, p = 0.0307) and increased SAT area (176.0 versus 188.0 cm^2, p = 0.0036) and, thus, a higher

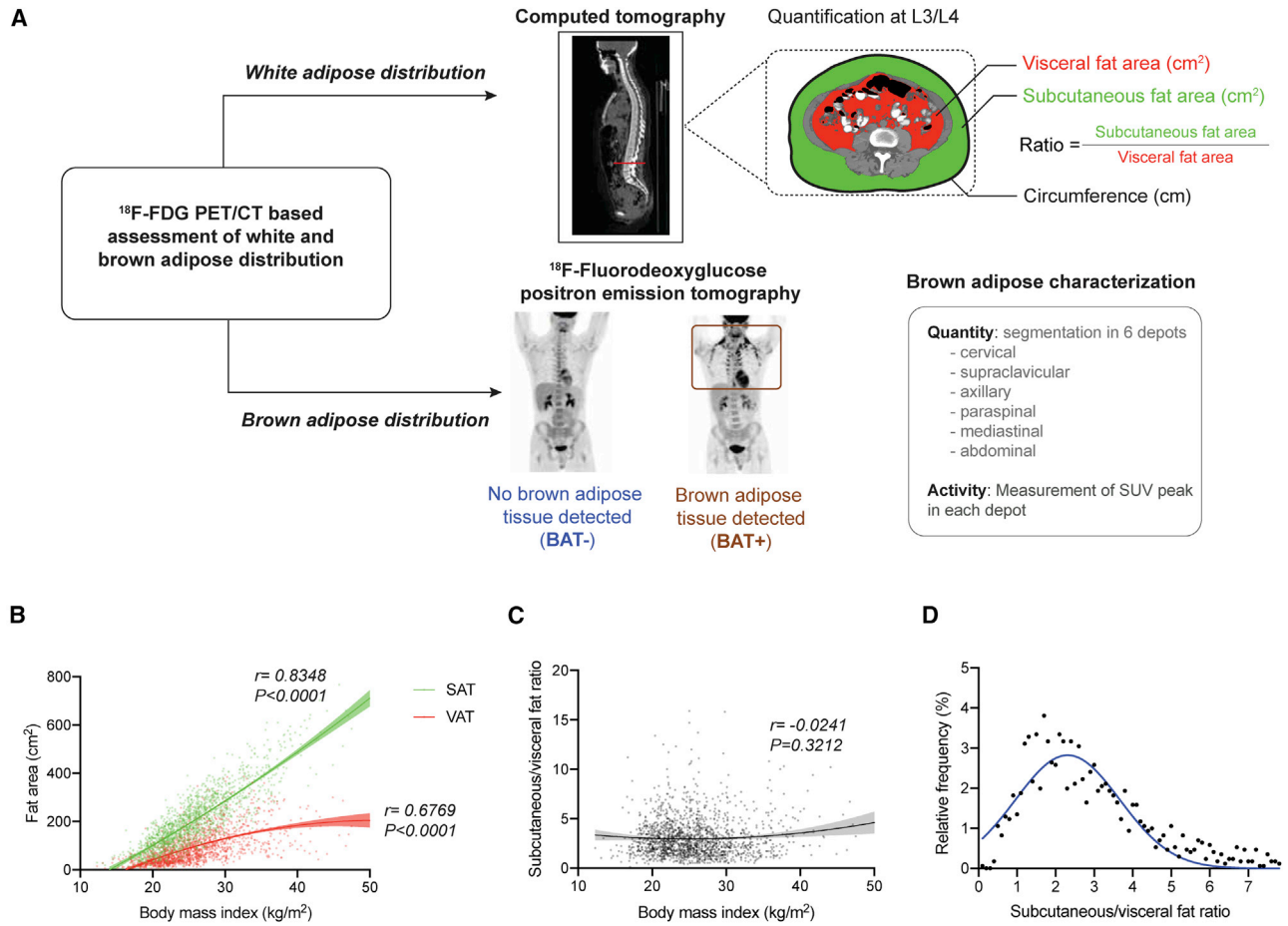

Figure 2. Illustration of ^{18}F-FDG PET/CT measurements and WAT distribution

(A) Schematic of WAT quantification on transverse CT slides at the L3/L4 level and detection and quantification of BAT by ^{18}F-FDG PET.

(B) Scatterplot depicting the correlation between BMI and VAT and SAT areas. Solid lines represent fitted curves derived from second-order polynomial equations, and shaded areas are 95% CIs. Correlation was assessed by calculating Spearman's rank correlation coefficient. Fitted curves are shown up to a BMI of 50 kg/m^2, and individual data points are depicted for 1,701 individuals.

(C) Scatterplot depicting the correlation between BMI and SAT:VAT ratio. The solid line represents the fitted curve derived from second-order polynomial equations, and shaded areas are 95% CIs. Correlation was assessed by calculating Spearman's rank correlation coefficient. The fitted curve is shown up to a BMI of 50 kg/m^2, and individual data points are depicted for 1,701 individuals.

(D) Scatterplot depicting the relative distribution of SAT:VAT ratio in our cohort. The solid blue line represents the fitted curve derived from second-order polynomial equations. The fitted curve is shown up to a SAT:VAT ratio of 7.8.

For (C) and (D), fitted curves were derived from measurements of 1,702 individuals.

SAT:VAT ratio (2.4 versus 2.7, $p < 0.0001$) (Figures 3A–3C; Table 1). These BAT-associated differences in WAT distribution were noted even independent of age, gender, and BMI (β-estimate −10.42, 95% confidence interval [CI] −14.60 to −6.25, $p < 0.0001$ for VAT; β-estimate 14.18, 95% CI 8.99–19.38, $p < 0.0001$ for SAT; Table S3) and were most pronounced at higher BMI values (β-estimate 0.03, 95% CI 0.00–0.06, $p = 0.0210$; Figures 3D and 3E).

Previous work reported that, in healthy individuals subjected to cold exposure before ^{18}F-FDG PET/CT, BAT activity was inversely correlated with visceral and, to a lesser extent, subcutaneous adiposity.[32] To assess whether the quantity or glucose uptake activity of BAT is associated with body fat distribution, we examined whether the number or FDG uptake intensity of BAT depots on PET/CT were correlated with WAT distribution. Interestingly, the number of active BAT depots was weakly inversely correlated with VAT area ($r = -0.1895$, $p < 0.0001$) and positively correlated with SAT:VAT ratio ($r = 0.2149$, $p < 0.0001$) but not significantly correlated with SAT area ($r = -0.0025$, $p = 0.4999$) (Figures 3F–3H). Peak BAT activity was negatively predictive of VAT area (β-estimate −2.78, 95% CI −4.02 to −1.55, $p < 0.0001$) and positively predictive of SAT:VAT ratio (β-estimate 0.14, 95% CI 0.10–0.18, $p < 0.0001$) but not of SAT area (β-estimate 2.22, 95% CI −0.16 to 4.61, $p = 0.0677$; Figures 3I and 3J). Our results thus support previous observations regarding associations between BAT activity and body fat distribution. Our work illustrates that, even without previous cold exposure, BAT activity correlates inversely with visceral

CellPress
OPEN ACCESS

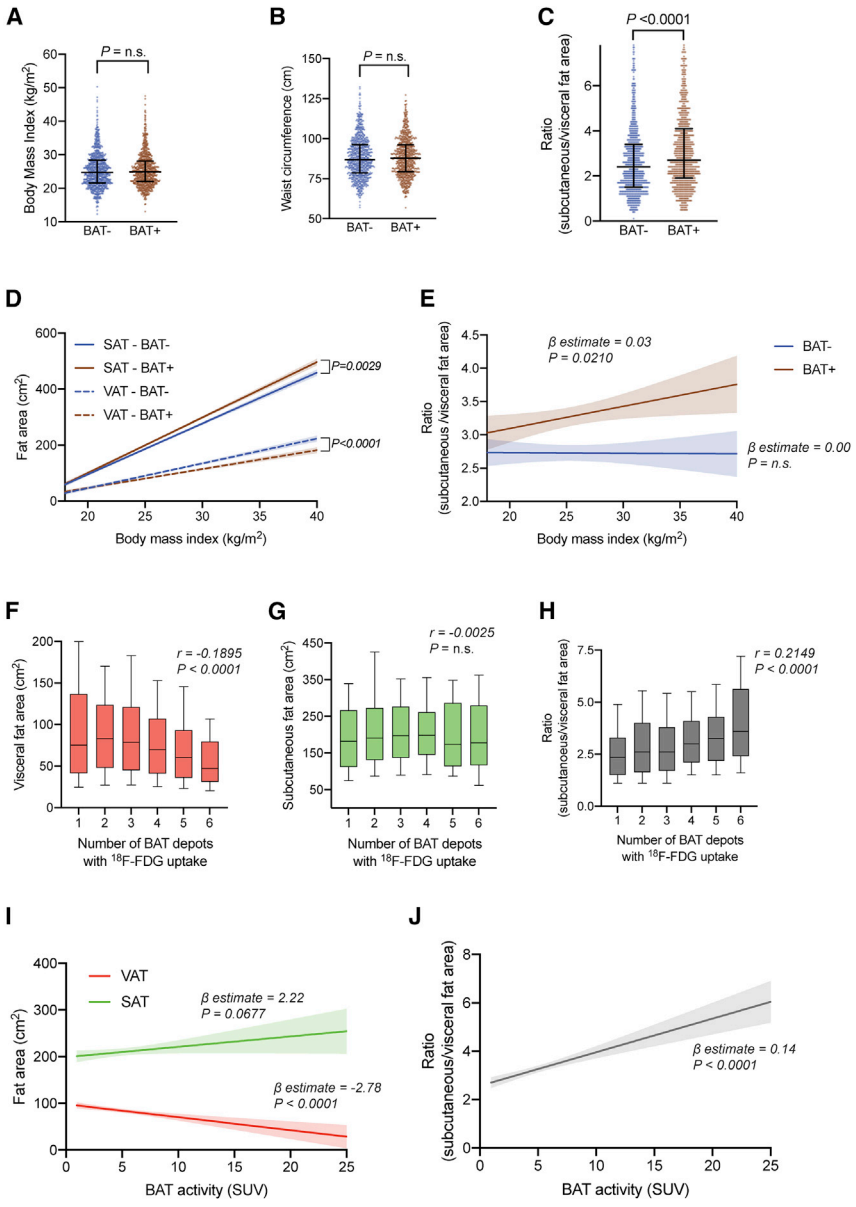

Figure 3. BAT status and activity are associated with body fat distribution

(A) Distribution of BMI by BAT status. Lines represent the 10th percentile, median, and 90th percentile. The p value was calculated based on a Mann-Whitney *U* test.

(B) Distribution of waist circumference on CT by BAT status. Lines represent the 10th percentile, median, and 90th percentile. The p value was calculated based on a Mann-Whitney *U* test.

(C) Distribution of SAT:VAT ratio by BAT status. Lines represent the 10th percentile, median, and 90th percentile. The p value was calculated based on a Mann-Whitney *U* test. The depicted data show measurements for 1,662 individuals.

(D) Best fit curves representing the relationship between BMI and SAT area (solid lines) or VAT area (dashed lines), stratified by BAT status, were calculated using linear regression analysis. The shaded areas represent the 95% CIs. The p values were calculated for assessing statistically significant differences between the slopes of these two lines. Best fit curves are shown up to a BMI of 40 kg/m^2.

(E) Best fit curves representing the relationship between BMI and SAT:VAT ratio, stratified by BAT status, were calculated using linear regression analysis. The shaded areas represent the 95% CIs. β-Estimates and p values correspond to the linear regression model. Best fit curves are shown up to a BMI of 40 kg/m^2.

(F) Boxplot of the total VAT area against the number of active BAT depots. Boxes represent the 25th percentile, median, and 75th percentile, and whiskers illustrate the 10th and 90th percentiles. Correlations were assessed by calculating Spearman's rank correlation coefficient.

(G) Boxplot of the total SAT area against the number of active BAT depots. Boxes represent the 25th percentile, median, and 75th percentile, and whiskers illustrate the 10th and 90th percentiles. Correlations were assessed by calculating Spearman's rank correlation coefficient.

(H) Boxplot of the SAT:VAT ratio against the number of active BAT depots. Boxes represent the 25th percentile, median, and 75th percentile, and whiskers illustrate the 10th and 90th percentiles. Correlations were assessed by calculating Spearman's rank correlation coefficient.

(I) Best fit curves of SAT and VAT areas as a function of BAT activity on PET/CT were calculated using linear regression analysis. The shaded areas represent the 95% CIs. β-Estimates and p values correspond to the linear regression model. Data are shown up to a BAT activity of 25 SUVs.

(J) Best fit curve of SAT:VAT ratio as a function of BAT activity on PET/CT was calculated using linear regression analysis. The shaded areas represent the 95% CIs. β-Estimate and p value correspond to the linear regression model. Data are shown up to a BAT activity of 25 SUVs.

For (A) and (B), data are shown for measurements of 1,702 individuals. For (D) and (E), fitted curves were derived from measurements of 1,702 individuals. For (F)–(H), data are shown for measurements of 856 patients. For (I) and (J), fitted curves are derived from measurements of 856 individuals.

adiposity. The discrepancy between our data and the data reported by Saito et al.[32] regarding the correlation of BAT activity and SAT area may be related to the differences in the study population and between cold-induced and retrospective identification of BAT on ^{18}F FDG PET/CT.

Prior studies have shown that age is correlated with decreased prevalence and activity of BAT[34,35] and increased quantity of VAT.[41–45] We thus used two multivariable analysis models to test whether SAT and VAT areas (model 1) or SAT:VAT ratio (model 2) can predict the number of BAT depots or BAT activity. These models were adjusted for age, gender, and BMI. We found no independent association between SAT, VAT, or SAT:VAT ratio and the number of BAT depots (Table S4). However, BAT activity was weakly negatively associated with VAT area (β-estimate −0.09, 95% CI −0.14 to −0.04, p = 0.0004) and positively associated with SAT:VAT ratio (β-estimate 0.25, 95% CI 0.13–0.36,

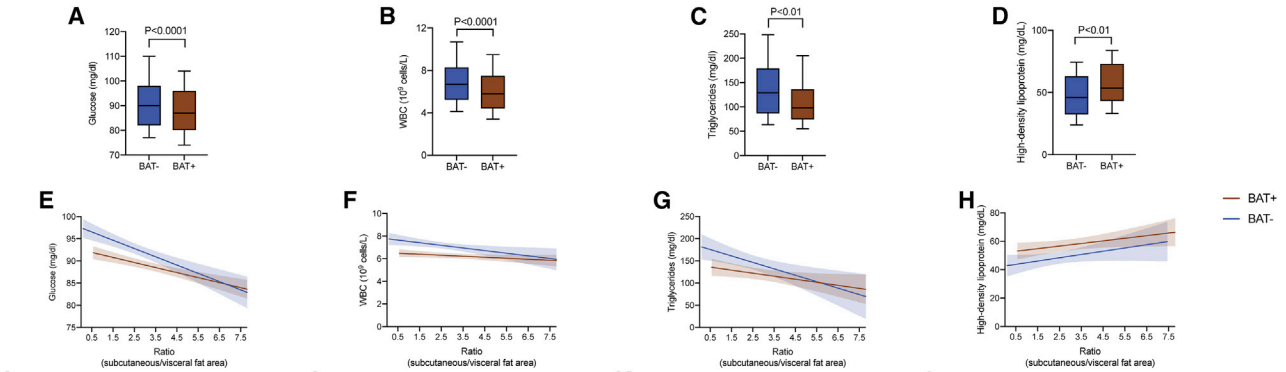

I

	Blood glucose		
	β-Estimate	95% CI	*P*-Value
Age (years)	0.11	0.06 – 0.16	<0.0001
Gender (female)	-2.60	-4.42 – (-0.77)	0.0054
BMI (kg/m²)	0.36	0.22 – 0.50	<0.0001
SAT/VAT ratio	-0.99	-1.42 – (-0.56)	<0.0001
BAT (present)	-3.04	-4.49 – (-1.60)	<0.0001

J

	White blood cell count		
	β-Estimate	95% CI	*P*-Value
Age (years)	0.01	0.00 – 0.03	0.0266
Gender (female)	-0.01	-0.47 – 0.44	0.9513
BMI (kg/m²)	0.04	0.00 – 0.07	0.0366
SAT/VAT ratio	-0.10	-0.21 – 0.00	0.5963
BAT (present)	-0.86	-1.21 – (-0.52)	<0.0001

K

	Triglycerides		
	β-Estimate	95% CI	*P*-Value
Age (years)	-0.72	-1.36 – (-0.09)	0.0250
Gender (female)	0.30	-22.98 – 23.57	0.9800
BMI (kg/m²)	1.81	-0.19 – 3.81	0.0759
SAT/VAT ratio	-12.04	-17.96 – (6.13)	<0.0001
BAT (present)	-23.33	-43.07 – (-3.58)	0.0208

L

	High density lipoprotein		
	β-Estimate	95% CI	*P*-Value
Age (years)	0.26	0.09 – 0.43	0.0036
Gender (female)	10.50	4.22 – 16.78	0.0012
BMI (kg/m²)	-1.01	-1.53 – (0.49)	0.0002
SAT/VAT ratio	2.29	0.65 – 3.81	0.0058
BAT (present)	8.97	3.66 – 14.28	0.0010

Figure 4. BAT is associated with improved metabolic parameters independent of SAT:VAT ratio

(A–D) Boxplots of glucose (A), WBCs (B), triglycerides (C), and HDL (D), stratified by BAT status. Boxes represent the 25th percentile, median, and 75th percentile, and whiskers illustrate the 10th and 90th percentiles. All p values were calculated based on a Mann-Whitney *U* test. The data depicted in (A) show measurements for 1,683 individuals, in (B) for 1,221 individuals, in (C) for 249 individuals, and in (D) for 209 individuals.

(E–H) Association between SAT:VAT ratio and levels of glucose (E), WBCs (F), triglycerides (G), or HDL (H), stratified by BAT status. Best fit curves were calculated using linear regression. The shaded areas represent the 95% CIs. Best fit curves were derived for (A) from measurements of 1,683 individuals, in (B) of 1,221 individuals, in (C) of 249 individuals, and in (D) of 209 individuals and are shown up to a SAT:VAT ratio of 7.8.

(I–L) Multivariable linear regression analysis adjusted for age, gender, BMI, SAT:VAT ratio, and BAT as predictors of levels of glucose (I), WBCs (J), triglycerides (K), or HDL (L) as outcome.

$p < 0.0001$) (Table S4). A trend toward a positive association between BAT activity and SAT area (β-estimate 0.04, 95% CI 0.00–0.08, $p = 0.0640$) was also noted (Table S4). These data suggest that BAT may mitigate central adiposity by decreasing VAT and increasing SAT in a dose-dependent manner.

BAT is associated with an improved metabolic profile, specifically in individuals with central obesity

We have previously shown that BAT is associated with improved cardiometabolic health.[25] Here we show that BAT is associated with improved body fat distribution, offering one possible explanation for our previous findings. To better characterize the extent to which BAT and WAT distribution conjointly affects metabolic function, we first examined the effect of these fat depots on laboratory metrics of metabolic health. We found that VAT was associated with higher blood glucose, WBC count, and triglycerides and lower HDL levels, whereas SAT was not associated or only weakly associated with these parameters (Figures S3A–S3D). The presence of BAT was associated with lower blood glucose, WBC count, and triglycerides and higher HDL (Figures 4A–4D). When stratified by SAT:VAT ratio, these associations were more pronounced in individuals with a lower SAT:VAT ratio (Figures 4E–4H). Last, the presence of BAT was associated independently with lower blood glucose, WBC count, and triglycerides and higher HDL after adjusting for age, gender, BMI, and SAT:VAT ratio (Figures 4I-4L). These data indicate that the beneficial metabolic effects associated with BAT can be explained partially by healthier body fat distribution and that BAT is also associated with additional benefits independent of body fat distribution.

BAT is associated with decreased liver fat and T2DM

To determine whether the observed associations between fat depots and laboratory metrics of metabolic health are associated with improved disease status, we next assessed liver fat accumulation on CT (Figure 5A). Lower liver parenchymal density on unenhanced CT, as quantified by lower Hounsfield units (HU), is an established surrogate for hepatic lipid accumulation.[46] Multivariable analysis showed that increased VAT is associated with lower liver density, indicating more liver fat, whereas SAT was associated with liver density, but this association was lost when adjusted for age, gender, and BMI (Table 2; Figure S3E). A lower SAT:VAT ratio was significantly associated with decreased liver density (β-estimate 0.73, 95% CI 0.49–0.97, $p < 0.0001$; Figure 5B). These results corroborate prior observations that central obesity is associated with increased liver fat accumulation.[47]

Additionally, individuals with BAT+ scans exhibited higher liver density compared with BAT− individuals (Figure 5C). This association was most pronounced in individuals with a low SAT:VAT ratio (Figure 5D) and remained significant after adjusting for age, gender, BMI, and SAT or VAT area (Table 2). These findings suggest that BAT is associated with attenuated liver fat accumulation, particularly in individuals with central adiposity, and that this observation is not solely explained by improved body fat distribution.

Similarly, BAT was associated with a decreased prevalence of T2DM ($p = 0.0012$) (Figure 5E).[25] Here, too, a lower VAT area ($r = -0.0085$, $p < 0.0001$) and a higher SAT:VAT ratio were associated with decreased prevalence of T2DM in all individuals (odds ratio [OR] 0.68, 95% CI 0.59–0.78, $p < 0.0001$) or in

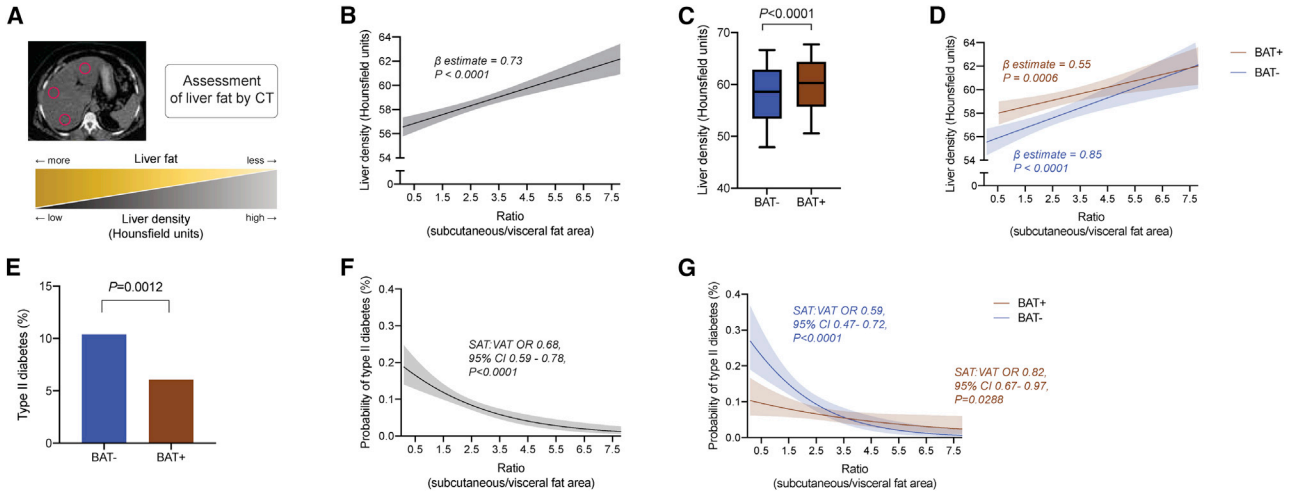

Figure 5. BAT is associated with improved markers of hepatic steatosis and T2DM

(A) Illustration of liver density (HU) measurement as a surrogate for fatty liver disease.

(B) Association of liver density based on HU measurements and SAT:VAT ratio. β-Estimate and p value were calculated using linear regression analysis. The best fit curve was derived from measurements of 1,298 individuals and is shown up to a SAT:VAT ratio of 7.8.

(C) Boxplot of mean liver HUs stratified by BAT status. Boxes represent the 25th percentile, median, and 75th percentile, and whiskers illustrate the 10th and 90th percentiles. The p value is calculated based on a Mann-Whitney *U* test. The depicted data show measurements for 1,298 individuals.

(D) Best fit curves of mean liver HUs across SAT:VAT ratios, stratified by BAT status, were calculated using linear regression analysis, and shaded areas depict 95% CIs. The best fit curves were derived from measurements of 1,298 individuals and are shown up to a SAT:VAT ratio of 7.8.

(E) Prevalence of T2DM stratified by BAT status. Data are shown for 1,702 individuals.

(F) Best fit curve of the probability of T2DM across SAT:VAT ratios was calculated using logistic regression analysis, and shaded area depicts the 95% CI. OR and p value correspond to the logistic regression model. The best fit curve was derived from measurements of 1,702 individuals and is shown up to a SAT:VAT ratio of 7.8.

(G) Best fit curves of the probability of T2DM across SAT:VAT ratios, stratified by BAT status, were calculated using logistic regression analysis, and shaded areas depict the 95% CI. ORs and p values correspond to the logistic regression model. The best fit curves were derived from measurements of 1,702 individuals and are shown up to a SAT:VAT ratio of 7.8.

BAT– (OR 0.59, 95% CI 0.47–0.72, p < 0.0001) or BAT+ (OR 0.82, 95% CI 0.67–0.97, p = 0.0288) individuals (Figures 5F, 5G, and S3F). The effect of BAT on this association was greatest at lower SAT:VAT ratios (Figure 5G). These data suggest that BAT has its most potent metabolic effects at unfavorably low SAT:VAT ratios (indicating a relative increase of VAT area compared with SAT area).

Last, we used a multivariable logistic regression model to adjust for the potential interaction between BAT, SAT, and VAT areas (in addition to other potential confounders, such as age, gender, and BMI) when determining the association between these factors and T2DM. Our results showed that BAT is associated with lower prevalence of T2DM (OR 0.60, 95% CI 0.41–0.86, p = 0.0066), whereas age (OR 1.04, 95% CI 1.03–1.06, p < 0.0001) and VAT area (OR 1.04, 95% CI 1.01–1.08, p = 0.0119) were associated with an increased OR of T2DM prevalence (Table 2). These results indicate that BAT has an effect on metabolic health independent of its association with a beneficial body fat distribution.

Conclusions

In conclusion, our data reveal that BAT is associated with decreased central adiposity, as indicated by a decrease in VAT and an increase in SAT and SAT:VAT ratio. This change in body fat distribution is associated with improved metabolic health[5,7–14] and may hence contribute to the metabolic benefits associated previously with BAT.[25,48] In addition, increased BAT activity and number of depots are associated with improvements in metabolic parameters, suggesting that not only the quantity but also the function of BAT may be of importance for WAT distribution.

Importantly, we observe that BAT retains its association with improved beneficial effects on blood glucose, LDL and HDL levels, liver fat accumulation, and T2DM independent of WAT distribution. Furthermore, these observations seem to be most pronounced in individuals with central adiposity. Although energy expenditure at rest has been linked previously to changes in body fat distribution,[49,50] the association of BAT with metabolic health independent of WAT distribution suggests that additional mechanisms may underlie the observed findings. As an example, potential endocrine factors secreted by BAT have been implicated as a mechanism that may explain how BAT contributes to metabolic health.[51] An intriguing association is that of BAT status and liver fat accumulation. Although a number of studies in rodents have linked BAT function to protection from hepatic steatosis,[52–54] this connection is less well established in humans.[48] The underlying mechanisms may include modulation of circulating fatty acid levels through BAT,[55] resulting in decreased lipotoxicity; BAT-secreted factors, such as neuregulin 4, that directly modulate hepatic metabolism;[52] or endocrine

Table 2. Multivariable regression models for predictors of liver density on CT (HU) and T2DM

	Liver HU			T2DM		
	β-Estimate	95% CI	p Value	OR	95% CI	p value
BAT	1.20	0.41 to 1.98	0.0027	0.60	0.41–0.86	0.0066
Age (year)	0.02	−0.01 to 0.05	0.1189	1.04	1.03–1.06	<0.0001
Gender (male)	0.24	−0.81 to 1.3	0.6515	1.21	0.76–1.89	0.4150
BMI (kg/m^2)	−0.09	−0.26 to 0.07	0.2711	1.05	0.97–1.13	0.2298
VAT (10 cm^2)	−0.43	−0.51 to −0.34	<0.0001	1.04	1.01–1.08	0.0119
SAT (10 cm^2)	−0.02	−0.09 to 0.05	0.6506	0.99	0.95–1.02	0.4036

interactions between BAT and other organs that indirectly influence hepatic lipid storage.

Finally, our findings suggest that BAT status and increased BAT activity in humans may ameliorate the severity of metabolic disease associated with obesity, particularly visceral adiposity. Our observation that not only the presence but also the activity of BAT are associated with decreased visceral adiposity supports a relationship between BAT and WAT distribution. Further research into the mechanisms underlying the observed associations between BAT and WAT distribution as well as a deeper understanding of how BAT modulates metabolic outcomes is necessary if we are to harness the therapeutic potential of this tissue to treat obesity and comorbid diseases.[1,2]

Limitations of study

This is a retrospective, observational study that reports associations. The study design does not allow one to make conclusions about cause-effect relationships between BAT and body fat distribution or metabolic health. Individuals in our study received ^{18}F-FDG PET/CT scans for cancer-associated diagnoses, treatment, or surveillance. Thus, it cannot be excluded that the underlying cancer type, stage, and treatment may have confounded our results. Furthermore, individuals were not cold stimulated prior to their ^{18}F-FDG PET/CT scans, resulting in sub-maximal BAT activation and, subsequently, detection. Impaired systemic insulin sensitivity may also reduce ^{18}F-FDG uptake in BAT and, thus, its detection on PET/CT scans. Moreover, body fat distribution was derived from one CT slice only, and this may not fully capture body fat distribution characteristics. Last, unenhanced CTs and laboratory parameters were only available for subgroups of the study cohort, which might have introduced bias (Table S5).

STAR★METHODS

Detailed methods are provided in the online version of this paper and include the following:

- KEY RESOURCES TABLE
- RESOURCE AVAILABILITY
  - Lead contact
  - Materials availability
  - Data and code availability
- METHOD DETAILS
  - Study design, data collection and patient selection
  - ^{18}F-FDG-PET/CT examinations
  - Identification of BAT and measurement of BAT activity
  - Measurement of body fat distribution
  - Assessment of liver density on CT
- QUANTIFICATION AND STATISTICAL ANALYSIS

SUPPLEMENTAL INFORMATION

Supplemental information can be found online at https://doi.org/10.1016/j.xcrm.2021.100332.

ACKNOWLEDGMENTS

We thank Chester Poon for expert IT support and data extraction. The graphical abstract was created with BioRender. T.B. was supported in part by the National Center for Advancing Translational Sciences, NIH, through Rockefeller University (UL1TR001866) and a Bernard L. Schwartz Award for physician-scientists from Rockefeller University. P.C. was supported by the Sinsheimer Foundation and the American Diabetes Association Pathway Program Accelerator Award (1-17-ACE-17). A.G.W., P.C.A., and H.S. were supported in part through NIH/NCI Cancer Center Support Grant P30 CA008748.

AUTHOR CONTRIBUTIONS

P.C., H.S., A.G.W., and T.B. designed and conceived the study. A.G.W., T.B., and P.C.A. acquired the data. A.G.W., T.B., M.E., A.C., C.S.J., R.V., H.S., and P.C. analyzed and interpreted the data. T.B., A.G.W., M.E., A.C., H.S., and P.C. wrote the manuscript with input from all authors.

DECLARATION OF INTERESTS

T.B. is currently an employee of Roche Diagnostics, Rotkreuz, Switzerland.

Received: December 27, 2020
Revised: March 25, 2021
Accepted: June 8, 2021
Published: July 7, 2021

REFERENCES

1. Hales, C.M., Carroll, M.D., Fryar, C.D., and Ogden, C.L. (2020). Prevalence of Obesity and Severe Obesity Among Adults: United States, 2017-2018. NCHS Data Brief (*360*), 1–8.
2. Ward, Z.J., Bleich, S.N., Cradock, A.L., Barrett, J.L., Giles, C.M., Flax, C., Long, M.W., and Gortmaker, S.L. (2019). Projected U.S. State-Level Prevalence of Adult Obesity and Severe Obesity. N. Engl. J. Med. *381*, 2440–2450.
3. Finkelstein, E.A., Trogdon, J.G., Cohen, J.W., and Dietz, W. (2009). Annual medical spending attributable to obesity: payer-and service-specific estimates. Health Aff. (Millwood) *28*, w822–w831.

4. Björntorp, P. (1974). Effects of age, sex, and clinical conditions on adipose tissue cellularity in man. Metabolism *23*, 1091–1102.

5. Lee, P., Smith, S., Linderman, J., Courville, A.B., Brychta, R.J., Dieckmann, W., Werner, C.D., Chen, K.Y., and Celi, F.S. (2014). Temperature-acclimated brown adipose tissue modulates insulin sensitivity in humans. Diabetes *63*, 3686–3698.

6. Porter, S.A., Massaro, J.M., Hoffmann, U., Vasan, R.S., O'Donnel, C.J., and Fox, C.S. (2009). Abdominal subcutaneous adipose tissue: a protective fat depot? Diabetes Care *32*, 1068–1075.

7. Yusuf, S., Hawken, S., Ounpuu, S., Bautista, L., Franzosi, M.G., Commerford, P., Lang, C.C., Rumboldt, Z., Onen, C.L., Lisheng, L., et al.; INTERHEART Study Investigators (2005). Obesity and the risk of myocardial infarction in 27,000 participants from 52 countries: a case-control study. Lancet *366*, 1640–1649.

8. Després, J.-P., Lemieux, I., Bergeron, J., Pibarot, P., Mathieu, P., Larose, E., Rodés-Cabau, J., Bertrand, O.F., and Poirier, P. (2008). Abdominal obesity and the metabolic syndrome: contribution to global cardiometabolic risk. Arterioscler. Thromb. Vasc. Biol. *28*, 1039–1049.

9. Bhaskaran, K., Douglas, I., Forbes, H., dos-Santos-Silva, I., Leon, D.A., and Smeeth, L. (2014). Body-mass index and risk of 22 specific cancers: a population-based cohort study of 5·24 million UK adults. Lancet *384*, 755–765.

10. Chan, J.M., Rimm, E.B., Colditz, G.A., Stampfer, M.J., and Willett, W.C. (1994). Obesity, fat distribution, and weight gain as risk factors for clinical diabetes in men. Diabetes Care *17*, 961–969.

11. Jayedi, A., Soltani, S., Zargar, M.S., Khan, T.A., and Shab-Bidar, S. (2020). Central fatness and risk of all cause mortality: systematic review and dose-response meta-analysis of 72 prospective cohort studies. BMJ *370*, m3324.

12. Medalie, J.H., Papier, C.M., Goldbourt, U., and Herman, J.B. (1975). Major factors in the development of diabetes mellitus in 10,000 men. Arch. Intern. Med. *135*, 811–817.

13. Shekelle, R.B., Shryock, A.M., Paul, O., Lepper, M., Stamler, J., Liu, S., and Raynor, W.J., Jr. (1981). Diet, serum cholesterol, and death from coronary heart disease. The Western Electric study. N. Engl. J. Med. *304*, 65–70.

14. Willett, W.C., Manson, J.E., Stampfer, M.J., Colditz, G.A., Rosner, B., Speizer, F.E., and Hennekens, C.H. (1995). Weight, weight change, and coronary heart disease in women. Risk within the 'normal' weight range. JAMA *273*, 461–465.

15. Cypess, A.M., Lehman, S., Williams, G., Tal, I., Rodman, D., Goldfine, A.B., Kuo, F.C., Palmer, E.L., Tseng, Y.-H., Doria, A., et al. (2009). Identification and importance of brown adipose tissue in adult humans. N. Engl. J. Med. *360*, 1509–1517.

16. Fraum, T.J., Crandall, J.P., Ludwig, D.R., Chen, S., Fowler, K.J., Laforest, R.A., Salter, A., Dehdashti, F., An, H., and Wahl, R.L. (2019). Repeatability of Quantitative Brown Adipose Tissue Imaging Metrics on Positron Emission Tomography with ^{18}F-Fluorodeoxyglucose in Humans. Cell Metab. *30*, 212–224.e4.

17. van Marken Lichtenbelt, W.D., Vanhommerig, J.W., Smulders, N.M., Drossaerts, J.M.A.F.L., Kemerink, G.J., Bouvy, N.D., Schrauwen, P., and Teule, G.J.J. (2009). Cold-activated brown adipose tissue in healthy men. N. Engl. J. Med. *360*, 1500–1508.

18. Virtanen, K.A., Lidell, M.E., Orava, J., Heglind, M., Westergren, R., Niemi, T., Taittonen, M., Laine, J., Savisto, N.-J., Enerbäck, S., and Nuutila, P. (2009). Functional brown adipose tissue in healthy adults. N. Engl. J. Med. *360*, 1518–1525.

19. Cannon, B., and Nedergaard, J. (2004). Brown adipose tissue: function and physiological significance. Physiol. Rev. *84*, 277–359.

20. Jacobsson, A., Stadler, U., Glotzer, M.A., and Kozak, L.P. (1985). Mitochondrial uncoupling protein from mouse brown fat. Molecular cloning, genetic mapping, and mRNA expression. J. Biol. Chem. *260*, 16250–16254.

21. Shabalina, I.G., Petrovic, N., de Jong, J.M.A., Kalinovich, A.V., Cannon, B., and Nedergaard, J. (2013). UCP1 in brite/beige adipose tissue mitochondria is functionally thermogenic. Cell Rep. *5*, 1196–1203.

22. Bartelt, A., Bruns, O.T., Reimer, R., Hohenberg, H., Ittrich, H., Peldschus, K., Kaul, M.G., Tromsdorf, U.I., Weller, H., Waurisch, C., et al. (2011). Brown adipose tissue activity controls triglyceride clearance. Nat. Med. *17*, 200–205.

23. Fedorenko, A., Lishko, P.V., and Kirichok, Y. (2012). Mechanism of fatty-acid-dependent UCP1 uncoupling in brown fat mitochondria. Cell *151*, 400–413.

24. Porter, C., Herndon, D.N., Chondronikola, M., Chao, T., Annamalai, P., Bhattarai, N., Saraf, M.K., Capek, K.D., Reidy, P.T., Daquinag, A.C., et al. (2016). Human and Mouse Brown Adipose Tissue Mitochondria Have Comparable UCP1 Function. Cell Metab. *24*, 246–255.

25. Becher, T., Palanisamy, S., Kramer, D.J., Eljalby, M., Marx, S.J., Wibmer, A.G., Butler, S.D., Jiang, C.S., Vaughan, R., Schöder, H., et al. (2021). Brown adipose tissue is associated with cardiometabolic health. Nat. Med. *27*, 58–65.

26. Orava, J., Nuutila, P., Lidell, M.E., Oikonen, V., Noponen, T., Viljanen, T., Scheinin, M., Taittonen, M., Niemi, T., Enerbäck, S., and Virtanen, K.A. (2011). Different metabolic responses of human brown adipose tissue to activation by cold and insulin. Cell Metab. *14*, 272–279.

27. Ouellet, V., Labbé, S.M., Blondin, D.P., Phoenix, S., Guérin, B., Haman, F., Turcotte, E.E., Richard, D., and Carpentier, A.C. (2012). Brown adipose tissue oxidative metabolism contributes to energy expenditure during acute cold exposure in humans. J. Clin. Invest. *122*, 545–552.

28. Yoneshiro, T., Aita, S., Matsushita, M., Kameya, T., Nakada, K., Kawai, Y., and Saito, M. (2011). Brown adipose tissue, whole-body energy expenditure, and thermogenesis in healthy adult men. Obesity (Silver Spring) *19*, 13–16.

29. Brendle, C., Werner, M.K., Schmadl, M., la Fougère, C., Nikolaou, K., Stefan, N., and Pfannenberg, C. (2018). Correlation of Brown Adipose Tissue with Other Body Fat Compartments and Patient Characteristics: A Retrospective Analysis in a Large Patient Cohort Using PET/CT. Acad. Radiol. *25*, 102–110.

30. Wang, Q., Zhang, M., Ning, G., Gu, W., Su, T., Xu, M., Li, B., and Wang, W. (2011). Brown adipose tissue in humans is activated by elevated plasma catecholamines levels and is inversely related to central obesity. PLoS ONE *6*, e21006.

31. Wang, Q., Zhang, M., Xu, M., Gu, W., Xi, Y., Qi, L., Li, B., and Wang, W. (2015). Brown adipose tissue activation is inversely related to central obesity and metabolic parameters in adult human. PLoS ONE *10*, e0123795.

32. Saito, M., Okamatsu-Ogura, Y., Matsushita, M., Watanabe, K., Yoneshiro, T., Nio-Kobayashi, J., Iwanaga, T., Miyagawa, M., Kameya, T., Nakada, K., et al. (2009). High incidence of metabolically active brown adipose tissue in healthy adult humans: effects of cold exposure and adiposity. Diabetes *58*, 1526–1531.

33. Chen, K.Y., Cypess, A.M., Laughlin, M.R., Haft, C.R., Hu, H.H., Bredella, M.A., Enerbäck, S., Kinahan, P.E., Lichtenbelt, W. van M., Lin, F.I., et al. (2016). Brown Adipose Reporting Criteria in Imaging STudies (BARCIST 1.0): Recommendations for Standardized FDG-PET/CT Experiments in Humans. Cell Metab. *24*, 210–222.

34. Cronin, C.G., Prakash, P., Daniels, G.H., Boland, G.W., Kalra, M.K., Halpern, E.F., Palmer, E.L., and Blake, M.A. (2012). Brown fat at PET/CT: correlation with patient characteristics. Radiology *263*, 836–842.

35. Steinberg, J.D., Vogel, W., and Vegt, E. (2017). Factors influencing brown fat activation in FDG PET/CT: a retrospective analysis of 15,000+ cases. Br. J. Radiol. *90*, 20170093.

36. Camhi, S.M., Bray, G.A., Bouchard, C., Greenway, F.L., Johnson, W.D., Newton, R.L., Ravussin, E., Ryan, D.H., Smith, S.R., and Katzmarzyk, P.T. (2011). The relationship of waist circumference and BMI to visceral,

subcutaneous, and total body fat: sex and race differences. Obesity (Silver Spring) *19*, 402–408.

37. Grundy, S.M., Neeland, I.J., Turer, A.T., and Vega, G.L. (2013). Waist circumference as measure of abdominal fat compartments. J. Obes. *2013*, 454285.
38. Kaess, B.M., Pedley, A., Massaro, J.M., Murabito, J., Hoffmann, U., and Fox, C.S. (2012). The ratio of visceral to subcutaneous fat, a metric of body fat distribution, is a unique correlate of cardiometabolic risk. Diabetologia *55*, 2622–2630.
39. Ladeiras-Lopes, R., Sampaio, F., Bettencourt, N., Fontes-Carvalho, R., Ferreira, N., Leite-Moreira, A., and Gama, V. (2017). The Ratio Between Visceral and Subcutaneous Abdominal Fat Assessed by Computed Tomography Is an Independent Predictor of Mortality and Cardiac Events. Rev. Esp. Cardiol. (Engl. Ed.) *70*, 331–337.
40. Kwon, H., Kim, D., and Kim, J.S. (2017). Body Fat Distribution and the Risk of Incident Metabolic Syndrome: A Longitudinal Cohort Study. Sci. Rep. *7*, 10955.
41. Borkan, G.A., Hults, D.E., Gerzof, S.G., Robbins, A.H., and Silbert, C.K. (1983). Age changes in body composition revealed by computed tomography. J. Gerontol. *38*, 673–677.
42. Hughes, V.A., Roubenoff, R., Wood, M., Frontera, W.R., Evans, W.J., and Fiatarone Singh, M.A. (2004). Anthropometric assessment of 10-y changes in body composition in the elderly. Am. J. Clin. Nutr. *80*, 475–482.
43. Lemieux, S., Prud'homme, D., Moorjani, S., Tremblay, A., Bouchard, C., Lupien, P.J., and Després, J.P. (1995). Do elevated levels of abdominal visceral adipose tissue contribute to age-related differences in plasma lipoprotein concentrations in men? Atherosclerosis *118*, 155–164.
44. Pascot, A., Lemieux, S., Lemieux, I., Prud'homme, D., Tremblay, A., Bouchard, C., Nadeau, A., Couillard, C., Tchernof, A., Bergeron, J., and Després, J.P. (1999). Age-related increase in visceral adipose tissue and body fat and the metabolic risk profile of premenopausal women. Diabetes Care *22*, 1471–1478.
45. Shimokata, H., Andres, R., Coon, P.J., Elahi, D., Muller, D.C., and Tobin, J.D. (1989). Studies in the distribution of body fat. II. Longitudinal effects of change in weight. Int. J. Obes. *13*, 455–464.
46. Kodama, Y., Ng, C.S., Wu, T.T., Ayers, G.D., Curley, S.A., Abdalla, E.K., Vauthey, J.N., and Charnsangavej, C. (2007). Comparison of CT methods for determining the fat content of the liver. AJR Am. J. Roentgenol. *188*, 1307–1312.
47. Pang, Q., Zhang, J.-Y., Song, S.-D., Qu, K., Xu, X.-S., Liu, S.-S., and Liu, C. (2015). Central obesity and nonalcoholic fatty liver disease risk after adjusting for body mass index. World J. Gastroenterol. *21*, 1650–1662.
48. Yilmaz, Y., Ones, T., Purnak, T., Ozguven, S., Kurt, R., Atug, O., Turoglu, H.T., and Imeryuz, N. (2011). Association between the presence of brown adipose tissue and non-alcoholic fatty liver disease in adult humans. Aliment. Pharmacol. Ther. *34*, 318–323.
49. Amdanee, N., Di, W., Liu, J., Yu, J., Sheng, Y., Lv, S., Chattun, M.R., Qi, H., Liu, W., Tang, L., and Ding, G. (2018). Age-associated changes of resting energy expenditure, body composition and fat distribution in Chinese Han males. Physiol. Rep. *6*, e13940.
50. Okura, T., Koda, M., Ando, F., Niino, N., and Shimokata, H. (2003). Relationships of resting energy expenditure with body fat distribution and abdominal fatness in Japanese population. J. Physiol. Anthropol. Appl. Human Sci. *22*, 47–52.
51. Villarroya, F., Cereijo, R., Villarroya, J., and Giralt, M. (2017). Brown adipose tissue as a secretory organ. Nat. Rev. Endocrinol. *13*, 26–35.
52. Wang, G.-X., Zhao, X.-Y., Meng, Z.-X., Kern, M., Dietrich, A., Chen, Z., Cozacov, Z., Zhou, D., Okunade, A.L., Su, X., et al. (2014). The brown fat-enriched secreted factor Nrg4 preserves metabolic homeostasis through attenuation of hepatic lipogenesis. Nat. Med. *20*, 1436–1443.
53. Shen, H., Jiang, L., Lin, J.D., Omary, M.B., and Rui, L. (2019). Brown fat activation mitigates alcohol-induced liver steatosis and injury in mice. J. Clin. Invest. *129*, 2305–2317.
54. Poekes, L., Gillard, J., Farrell, G.C., Horsmans, Y., and Leclercq, I.A. (2019). Activation of brown adipose tissue enhances the efficacy of caloric restriction for treatment of nonalcoholic steatohepatitis. Lab. Invest. *99*, 4–16.
55. Blondin, D.P., Tingelstad, H.C., Noll, C., Frisch, F., Phoenix, S., Guérin, B., Turcotte, É.E., Richard, D., Haman, F., and Carpentier, A.C. (2017). Dietary fatty acid metabolism of brown adipose tissue in cold-acclimated men. Nat. Commun. *8*, 14146.
56. Leitner, B.P., Huang, S., Brychta, R.J., Duckworth, C.J., Baskin, A.S., McGehee, S., Tal, I., Dieckmann, W., Gupta, G., Kolodny, G.M., et al. (2017). Mapping of human brown adipose tissue in lean and obese young men. Proc. Natl. Acad. Sci. USA *114*, 8649–8654.
57. Irlbeck, T., Massaro, J.M., Bamberg, F., O'Donnell, C.J., Hoffmann, U., and Fox, C.S. (2010). Association between single-slice measurements of visceral and abdominal subcutaneous adipose tissue with volumetric measurements: the Framingham Heart Study. Int. J. Obes. *34*, 781–787.

STAR★METHODS

KEY RESOURCES TABLE

REAGENT or RESOURCE	SOURCE	IDENTIFIER
Software and algorithms		
Prism (version 9.0.0)	GraphPad Software	https://www.graphpad.com/scientific-software/prism/
SAS (version 9.4)	SAS Institute	https://www.sas.com/en_us/software/viya.html
Adobe Illustrator CC (2019)	Adobe	https://www.adobe.com/
Aquarius iNtuition (version 4.4.13)	TeraRecon	https://www.terarecon.com/

RESOURCE AVAILABILITY

Lead contact

Requests for additional information, resources and reagents should be directed to the Lead Contact, Paul Cohen (pcohen@rockefeller.edu).

Materials availability

No new reagents or materials were generated in this study.

Data and code availability

Anonymized clinical data related to this study are available upon request. All requests are subject to an internal review by T.B., P.C., A.G.W. and H.S. and completion of a data sharing agreement, in accordance with the Rockefeller University and Memorial Sloan Kettering Cancer Center Institutional Review Board and Institutional Guidelines.

METHOD DETAILS

Study design, data collection and patient selection

The current study was designed as a retrospective, single-center cross-sectional case/control study conducted at Memorial Sloan Kettering Cancer Center (MSKCC). The requirement for informed consent was waived due to its retrospective nature, and the study followed institutional guidelines and was approved by the Institutional Review Boards of The Rockefeller University and MSKCC.

Demographic and clinical characteristics, laboratory tests, and diagnosis codes based on the International Classification of Disease (9^{th} and 10^{th} editions) were extracted from electronic medical records using a standardized data collection method, as previously described.[25] The laboratory tests included blood glucose measured at the day of the ^{18}F-FDG-PET/CT after a fasting interval of at least 4-6 hours, white blood cell count (obtained if measured within three months of the PET/CT) and lipid profile (obtained if measured within one year of the PET/CT). ICD codes were used to categorize relevant diseases as previously described.[25]

A propensity-score matched cohort was established as described below. Of these 1,702 individuals, lab data were available as follows: blood glucose levels were available for 1,683 (98.88%) individuals, LDL and HDL levels were available for 209 (12.28%) individuals, triglycerides for 249 (14.63%) individuals, and total cholesterol for 229 (13.45%) individuals (Table S5). White blood cells (WBC) count was available for 1,645 (96.65%) individuals overall and for 1,221 (96.29%) of 1,268 individuals without a hematologic malignancy (Table S5). Girth measurements were available for 74 individuals (4.35%) (Table S5). Liver density measurements were performed for 1,298 (76.26%) individuals and omitted on 350 (20.56%) contrast-enhanced CT scans and 54 (3.17%) scans due to imaging artifacts or prior major liver resections (Table S5).

^{18}F-FDG-PET/CT examinations

^{18}F-FDG-PET/CT examinations were performed on a hybrid PET/CT scanner (Discovery series; GE Healthcare, Milwaukee, WI) after intravenous injection of approximately 444 MBq of ^{18}F-FDG. The radiotracer was obtained from a commercial source (IBA Molecular, Reston, VA) and calibrated by the MSKCC in-house radiopharmacy. ^{18}F-FDG was administered after an approximately 6-hour-long fasting period, and the time interval between tracer injection and imaging was approximately 60 minutes. For anatomic correlation and attenuation correction, free-breathing low-dose CT was performed with a tube voltage of 120–140 kV, a tube current of 80 mA, a pitch factor of 0.75-1.75, and a slice thickness of 3.75 mm.

Standardized uptake value (SUV) was used to quantify FDG uptake of BAT as a surrogate of its glucose uptake activity and was calculated as the ratio of a voxel's radioactivity concentration [kBq/mL] and the decay-corrected and body weight adjusted injected radiotracer activity [kBq/g] and reported as g/mL.

Identification of BAT and measurement of BAT activity

Identification of BAT and measurement of BAT activity was performed as previously described.[25] Briefly, 6 adipose regions of interest (ROIs) —namely cervical, supraclavicular, axillary, mediastinal, paraspinal and abdominal—were defined based on anatomical landmarks and CT characteristic of adipose tissue.[33,56] An SUV threshold of $\geq$ 1.5 g/mL, normalized to body mass, was used to identify BAT. BAT activity was reported as peak SUV value, measured as the average SUV within a 1 cm^3 sphere centered on the voxel with the highest ^{18}F-FDG uptake in each of the six adipose depots.

Measurement of body fat distribution

Image analyses were performed using commercially available software (Aquarius iNtuition version 4.4.13.; TeraRecon; Foster City, CA). Areas of VAT and SAT (CT density range: −195 to −45 HU) as well as the outer body circumference were semi-automatically measured in the transverse plane between the vertebral bodies L3/4. Two-dimensional measurements at this level were previously shown to be most strongly correlated with abdominal fat volumes and associated with cardiometabolic risk factors in a cohort of the Framingham Heart Study.[57]

Assessment of liver density on CT

For liver density measurements, circular regions of interests (approximate area: 5 cm^2) were placed at the level of the porta hepatis in the right posterior, right anterior, and left lateral hepatic segments, respectively (Figure 5A). Lower liver density on unenhanced CT, as quantified by HU, is a reliable surrogate of hepatic fat content.[46] Liver density was not measured on contrast-enhanced scans (n = 350) or cases with imaging artifacts or prior major liver resections (n = 54).

QUANTIFICATION AND STATISTICAL ANALYSIS

Continuous variables with non-normal distributions were expressed as median [IQR]. Categorical variables were expressed as number and percentage (%). Comparisons between groups were performed with Mann-Whitney U test for nonparametric variables and Fisher's exact test or chi-square test for categorical variables. Correlations between BMI and VAT or SAT area were assessed using Spearman's rank correlation coefficient. Non-linear regression curves were derived from second order polynomial curve fitting. Propensity scores were estimated using a non-parsimonious multivariable logistic-regression model with brown adipose tissue status (presence or absence) as the dependent variable and age, gender, BMI, and temperature at time of scan as covariates. Matching was performed using a greedy nearest neighbor matching algorithm without replacement with a caliper width set to 0.2 and a matching ratio of 1:1. Standardized difference means were used to assess balance before and after matching (Figure S1). Matching was conducted in SAS (version 9.4, SAS Institute, Cary, NC) using the **psmatch** function. All WBC count analyses were done using values from individuals without hematologic malignancies. A two-sided p value of less than 0.05 was used to define statistical significance for all tests. Data were analyzed in Prism (version 8.4.3, GraphPad Software, La Jolla, CA, USA) and SAS (version 9.4, SAS Institute, Cary, NC, USA).